Spectroscopy 22 (2008) 371–386
DOI 10.3233/SPE-2008-0360
IOS Press

Identification between *Stephania tetrandra* S. Moore and *Stephania cepharantha* Hayata by CWT–FTIR–RBFNN

Chang-Jiang Zhang [a,*] and Cun-Gui Cheng [b]

[a] *College of Mathematics, Physics and Information Engineering, Zhejiang Normal University, Jinhua 321004, China*

[b] *College of Chemistry and Life Science, Zhejiang Normal University, Jinhua 321004, China*

Abstract. Horizontal attenuation total reflection–Fourier transform infrared spectroscopy (HATR–FTIR) is used to measure the FTIR of *Stephania tetrandra* S. Moore and *Stephania cepharantha* Hayata. Because they belong to the same family and the same genus Chinese traditional medicinal materials, their chemical components are very similar. In order to extrude the difference between *Stephania tetrandra* S. Moore and *Stephania cepharantha* Hayata, continuous wavelet transform (CWT) is used to decompose the FTIR of *Stephania tetrandra* S. Moore and *Stephania cepharantha* Hayata. Three main scales are selected as the feature extracting space in the CWT domain. According the distribution of FTIR of *Stephania tetrandra* S. Moore and *Stephania cepharantha* Hayata, three feature regions are determined at every spectra band at selected three scales in the CWT domain. Thus nine feature parameters form the feature vector. The feature vector is input to the radius basis function neural network (RBFNN) to train so as to accurately classify the *Stephania tetrandra* S. Moore and *Stephania cepharantha* Hayata. 128 couples of FTIR are used to train and test the proposed method, where 78 couples of data are used as training samples and 50 couples of data are used as testing samples. Experimental results show that the accurate recognition rate between *Stephania tetrandra* S. Moore and *Stephania cepharantha* Hayata is respectively 99.8 and 99.9% by using the proposed method.

Keywords: Fourier transform infrared spectroscopy, continuous wavelet transform, radius basis function neural network, *Stephania tetrandra* S. Moore, *Stephania cepharantha* Hayata

1. Introduction

Fourier transform infrared spectroscopy method is a very common analysis tool with high sensitivity, resolution and fast speed, which has been widely used in the identification of Chinese traditional medicinal materials [1–3]. Because the traditional Chinese medicinal material is a kind of compound, the directly measured infrared spectrum is the superposition of all the infrared spectrums. Therefore, if general analysis method is used, this will greatly depend on the experience [4,5].

The wavelet transform is being used in chemistry and its related domain in recent years [6–11]. Ehrentreich pointed out that the wavelet transform has been established with the Fourier transform as a data-processing method in analytical chemistry [6]. Most of existing methods in chemistry are based on discrete wavelet transform [7,8]. For example, Shao et al. introduced the wavelet transform its applications in respect of photoacoustic spectroscopy, EXAFS spectrum, NMR analysis and Raman spectrum [7]. Ying et al. showed a typical example (apple NIR spectra) how wavelet transforms could be used in

* Corresponding author: Tel.: +86 579 82282501; E-mail: zcj74922@zjnu.cn.

order to extract quantitative information [8]. The sugar content of intact apple was measured by NIRS and analyzed by wavelet transform. Some researchers also used continuous wavelet transform to analyze the signal of chemistry [9]. For example, Lei et al. proposed a novel method of calculating approximate derivative of signals in analytical chemistry by using the continuous wavelet transform (CWT) [9]. In recent years, some researchers also combine the wavelet transform with other some intelligent technique to analyze the signal of chemistry [10,11]. For example, Khayamian et al. developed a wavelet neural network (WNN) model in quantitative structure property relationship (QSPR) for predicting solubility of 25 anthraquinone dyes in supercritical carbon dioxide over a wide range of pressures (70–770 bar) and temperatures (291–423 K) [10]. Piotrowski et al. developed a computational approach for performing efficient and reasonably accurate toxicity evaluation and prediction based on neural network and wavelet [11].

The advantages of the continuous wavelet transform (CWT) in the singularity detection of a signal are obvious. Compared with the discrete wavelet transform, it can detect the faint signal changes, which cannot be well implemented by discrete wavelet transform [12]. Artificial neural network can learn and train the information samples so that it will have similar memories of the human brain, identification capabilities and the implementation of various information processing functions. It has good self-learning, adaptive, associative memory, parallel processing and nonlinear conversion capabilities, which avoids complicated mathematical derivation. Even in the sample of the defect and parameter drift circumstances, the output can guarantee to be stable, thus it facilitates the theoretical analysis [12].

Stephania tetrandra S. Moore is a kind of commonly used Chinese traditional medicinal material, which can cure dropsy and ache. Because of much clinical usage, as well as proprietary Chinese traditional medicine preparations and chemical composition of extraction, and so on, this results in shortage of medicine, prices rising and chaos of varieties. Recently we discover that some *Stephania cepharantha* Hayata's roots have been mixed into *Stephania tetrandra* S. Moore. This paper uses HATR–FTIR method determines samples of *Stephania tetrandra* S. Moore and *Stephania cepharantha* Hayata directly. As *Stephania tetrandra* S. Moore and *Stephania cepharantha* Hayata belongs to sibling species, which contain the similar chemical composition, thus FTIR spectrums of theirs are also similar. If we use only FTIR spectra to identify them, this will be very difficult. Therefore, based on our previous work [13,14], we use the CWT to extract the features of both of the FTIR spectra. Then we use RBF neural network to efficiently identify them. Experimental results show that this obtains a good result.

2. CWT and RBF neural network

2.1. Continuous wavelet transform

In recent years, the wavelet transform becomes a powerful tool in the field of signal processing. Its basic idea is that a signal is mapped to a family of basic functions, which are constructed by the stretching and translation of "analysis-wavelet" [15]. This transformation is irreversible, and the signal can be carried out by the wavelet transform coefficient Reconstruction. Wavelet transform is divided into continuous wavelet transform and discrete wavelet transform (DWT), of which the discrete wavelet transform most is commonly used, it is mainly based on multi-resolution analysis and can be described in the form of digital filter. DWT can construct orthogonal wavelet basis and has a large number of extended forms. It can be used in the coding and data compression as a very economical and practical method. CWT is based on group theory, it is more flexible, and often can extract specific useful information of the signals.

DWT is based on the binary fixed grid, after having selected a proper wavelet, it exists multi-resolution analysis and orthogonal basis. CWT is a multi-scale description, and does not exist orthogonal basis.

Now most popular methods, which based on the wavelet transform to detect the singularity of the signal, are mostly based on discrete orthogonal wavelet transform, dyadic wavelet and the spline wavelet. In essence, they are all based on wavelet coefficients modulus maximum and zero cross approach. Although kinds of methods have been proposed, the ability to detect the faint signal is poor. This is mainly determined by the nature of DWT. Compared with several classic wavelet transforms, CWT will be more effective in the singularity detection of weak signals. It has a greater advantage in detecting singularity of the signal. The distinction of Fourier infrared spectrum between *Stephania tetrandra* S. Moore and *Stephania cepharantha* Hayata is not particularly obvious. If the Fourier transform infrared spectrum is directly used to distinguish *Stephania tetrandra* S. Moore and *Stephania cepharantha* Hayata, this will result in misjudgments. One-dimension CWT is implemented to their Fourier transform infrared spectrum. Under different resolutions we enlarge the differences between them to effectively identify *Stephania tetrandra* S. Moore and *Stephania cepharantha* Hayata. At the same time we extract representative nine continuous wavelet features of three scales, which are input to RBF neural network to efficiently identify *Stephania tetrandra* S. Moore and *Stephania cepharantha* Hayata.

2.2. RBF neural network

RBF (radial basis function) neural network can extend or pre-process the input vector to the high-dimensional space. It not only has good generalization ability, and also avoids the complex computation as back-propagation neural network. Therefore, we can achieve the rapid learning of neural network [16]. In this paper, we aim at the classification and identification to two kinds of plants (*Stephania tetrandra* S. Moore and *Stephania cepharantha* Hayata). Nine feature parameters are used as input vector, thus the input layer of the network needs nine neurons. Therefore, the RBF network has nine input neural units and two output neural units. Structure of RBF network is shown in Fig. 1.

The first layer is the input layer, it introduces eigenvector $\{S_1, S_2, \ldots, S_9\}$ into the network. The second layer is hidden layer, which is fully connected with the input layer (weight value $= 1$). Its role is equal to a conversion to the input modes, which transforms low-dimensional model input data to the

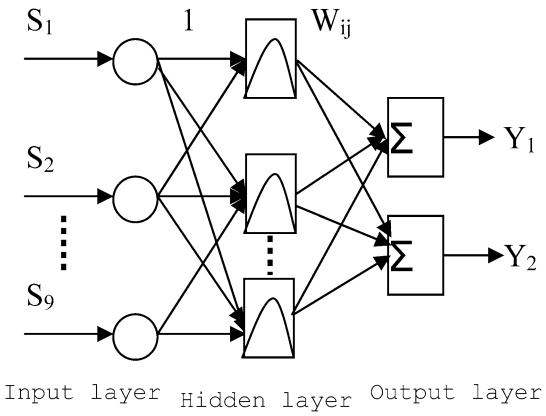

Fig. 1. Structure of RBF neural network.

high-dimensional space, to be in favor of the output layer's classification and recognition. Hidden layer node selects basis function as a transfer function. We use Gaussian function as follows:

$$\phi(x,\rho) = \exp\left[-(s-C_h)^2/\rho^2\right], \tag{1}$$

where: C_h is the center of basis functions, ρ is the width. Nodes compute the Euclidian distance between the input vector and the center, then transformation is carried out by the transfer function. The third layer is the output layer, output node j can be written as:

$$y_j = \sum W_{ij}\phi_i(\|s-C_h\|,\rho), \tag{2}$$

where: $h = 1, 2, \ldots, H$; $\|\cdot\|$ is Euclidean norm.

Radial basis function neural network has two adjustable parameters: center C_h and W_{ij}. The learning process of the network is divided into two stages: the first stage is the center adjustment, that is to say, the center C_h of Gaussian function of hidden layer's nodes is decided by the training sample; the second stage is the network weight value adjustment, that is to say, after having determined the parameters of hidden layer, we can get the output layer network's connecting weights W_{ij} with least squares principle according to the given training samples.

2.2.1. Center-adjusted algorithm

Center-adjusted algorithm uses the least clustering distance as index, and divides the input data sets into H classes and gets H centers. The steps of the algorithm are as follows:

(1) Select the initial center $C_h(0)$, $1 \leqslant h \leqslant H$ randomly, set the initial learning rate $\alpha(0)$;
(2) Calculate the minimum distance of kth step:

$$l_h(k) = \|s(k) - C_h(k-1)\|, \quad 1 \leqslant h \leqslant H. \tag{3}$$

(3) Find node q which has the minimum distance:

$$q = \arg[\min l_h(k)], \quad 1 \leqslant h \leqslant H. \tag{4}$$

(4) Update the center:

$$\begin{aligned} &C_h(k) = C_h(k-1), \quad 1 \leqslant h \leqslant H, h \neq q, \\ &C_q(k) = C_q(k-1) + \alpha(k)[x(k) - C_q(k-1)]. \end{aligned} \tag{5}$$

(5) Recalculation of the qth node's distance:

$$l_q(k) = \|x(k) - C_q(k-1)\|. \tag{6}$$

(6) Modify the learning rate:

$$\alpha(k+1) = \frac{\alpha(k)}{1 + \text{int}[k/H]^{1/2}}. \tag{7}$$

(7) $k = k + 1$, return to (2).

2.2.2. Adjustment algorithm of network weight values

The weight values can be seen as a vector

$$W_j(k) = [W_{1j}(k), W_{2j}(k), \ldots, W_{Hj}(k)]^{\mathrm{T}}, \quad 1 \leqslant j \leqslant N. \tag{8}$$

At the kth step, if the output vector of middle layer is:

$$\Phi(k) = [\Phi_1(k), \Phi_2(k), \ldots, \Phi_H(k)]^{\mathrm{T}} = [\Phi_1(l_1(k), \rho), \ldots, \Phi_H(l_H(k), \rho)]^{\mathrm{T}}. \tag{9}$$

The estimating output of step k is:

$$\hat{y}_j(k) = \sum W_{ij} \ddot{O}_i(l_i(k), \rho). \tag{10}$$

If the actual output is $y_j(k)$, the error is $\varepsilon_j(k) = y_j(k) - \hat{y}_j(k)$. According to recursive least squares method, adjusted algorithm of the network weight values is as follows:

$$W_j(k+1) = W_j(k) + P(k)\Phi(k) \cdot \varepsilon_j(k), \tag{11}$$

$$P(k) = \frac{1}{\lambda(k)}\left[P(k-1) - \frac{P(k-1)\Phi(k) \cdot \Phi^{\mathrm{T}}(k) \cdot P(k-1)}{\lambda(k) + \Phi^{\mathrm{T}}(k)P(k-1)\Phi(k)}\right], \tag{12}$$

where P is the error variance matrix and λ is a forgetting factor. To make the network identify samples more accurate, we can design a competition layer after the output layer in the network. The output vector of the competition layer consists of the output of all the neurons in the competition layer. The outputs of all other neurons are all zero except the victorious one.

3. Apparatus and materials

3.1. Apparatus

A Nicolet (Madison, WI, USA) NEXUS 670 TTIR Spectrometer, equipped with a temperature-stabilised deuterated tryglycine sulphate (DGTS) detector, a single-bounce horizontal attenuation total reflection (HATR) accessory, spectral range 4000–650 cm^{-1}, resolution 2 cm^{-1}, the cumulative number of scan 64 times.

3.2. Materials

Stephania tetrandra S. Moore and *Stephania cepharantha* Hayata are derived from Jinhua, Zhejiang province, China, in July 2007. All samples were deposited at the Department of Botany of Zhejiang Normal University in China. All samples have been grounded to fine powder in agate mortars to 200 mesh, respectively.

3.3. Spectral measurements

All spectra were recorded as 64 scans with 2 cm^{-1} resolution. The FTIR spectrum background was recorded before collecting the sample's FTIR spectrum. Reference spectra were recorded using a blank HATR germanium wafer. Single beam spectra were obtained for all the samples and ratioed against the background spectra of air to present the spectra in absorbance units. The powder sample was put on germanium wafer, and then impacted using pressure tower. FTIR were collected according to the instrument test requirement. After each experiment the HATR germanium wafer was thoroughly washed with distilled water and dried with nitrogen, and its spectra were examined to ensure that no residue from the previous experiment was retained on the germanium wafer surface. The powder samples cover the whole area of the HATR element that contributes to the spectral measurement. All spectra were automatic baseline corrected. All experiments were repeated three times and the averaged spectra used for further analysis.

3.4. Data analysis

FTIR of all the samples can be obtained by determination. According to the absorbance value characteristic of absorption peak, we can make the principal component analysis to the data, which are obtained by data copy in different wave bands. Then Matlab software is used to make wavelet transform to further analyze the data. Using Morlet wavelet, which has a good detection capability of the signal singularity, as the analysis wavelet, one-dimensional CWT is done to the FTIR spectra of samples under different scales. Then the difference of FTIR spectra of the samples in various scales is compared. We choose three representative scales to extract features of *Stephania tetrandra* S. Moore and *Stephania cepharantha* Hayata, then use RBF neural network to identify them. In the experiment we make one-dimensional CWT to the FTIR spectra of the samples (they are decomposed into 15 levels). We choose three scales (13, 9 and 5) as the scales to extract the feature vector.

4. Results and analysis

4.1. Analysis of FTIR

Figure 2 shows the FTIR spectra of *Stephania tetrandra* S. Moore and *Stephania cepharantha* Hayata. As can be seen from the Fig. 2, the main difference between them in 2900–3000 cm^{-1}. *Stephania tetrandra* S. Moore has an absorption peak in 2928 cm^{-1}, and *Stephania cepharantha* Hayata here has double peaks, which are in 2971 cm^{-1} and 2922 cm^{-1}, respectively. As *Stephania tetrandra* S. Moore and *Stephania cepharantha* Hayata are sibling species, they contain similar chemical composition so the distinction of their absorption peaks in the FTIR spectra is not very clear.

4.2. Principal component analysis

Principal component analysis (PCA) is made to the FTIR spectra of the samples. PCA load matrix CL can be obtained by principal component scores matrix C, eigenvalue λ and variance matrix S. Principal component load reflects the correlation between the principal component and the original FTIR variables. PCA case scores are used to draw 2-dimensional graph, the result is shown in Fig. 3. Figure 3 shows the impact of various indexes, that is the main component load. Horizontal coordinate shows the

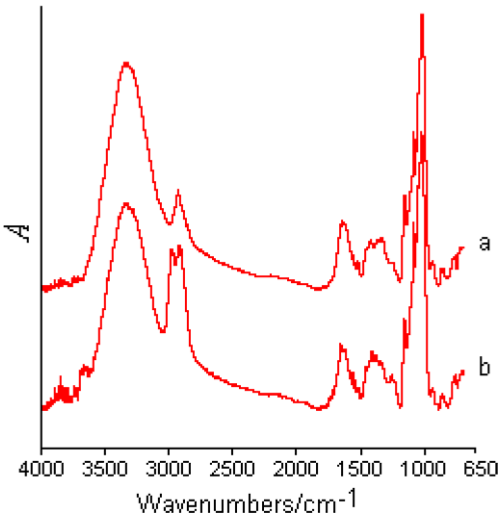

Fig. 2. FTIR spectra of (a) *Stephania tetrandra* S. Moore and (b) *Stephania cepharantha* Hayata.

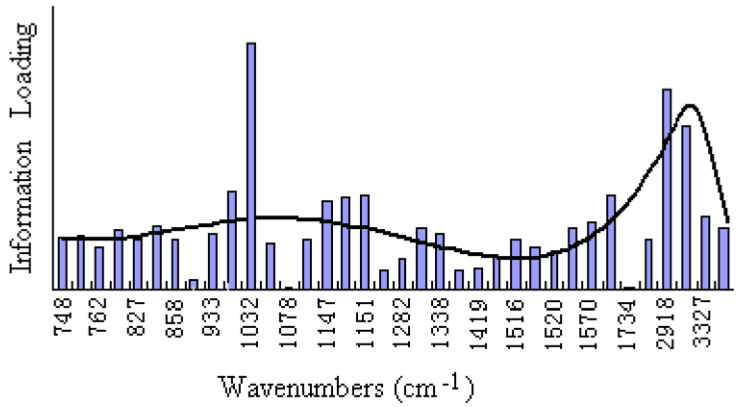

Fig. 3. PCA case scores by FTIR of *Stephania tetrandra* S. Moore and *Stephania cepharantha* Hayata samples.

wave number values of various indexes, and longitudinal coordinate is the impact factor values (PCA case scores).

Figure 3 shows that the biggest factor affecting the sample is the stretching vibration absorption band about 1050 cm^{-1} in the C–O bond of cellulose molecules. It also can be seen from Principal component analysis map the information load distribution, where larger information load region is in 1800–750 cm^{-1}. Characteristic in the area is not obvious because this region includes fingerprint area, which contains abundant molecular structure information, and in the high-wave-number absorption region is mainly hydroxyl and amino stretching vibration absorption. Therefore, this paper we extract wavelet features in the region of 1800–750 cm^{-1} and analyze them using artificial neural network.

4.3. Feature extraction of FTIR in CWT domain

When using wavelet transformation to analyze data, proper wavelet basis function and decomposing level number should be determined according to the spectral characteristics of the signal. The suitable

wavelet base and wavelet scale are determined by the effect of signal decomposition in different scales and the characteristics of the FTIR signal in wavelet multi-scale decomposition procedure. There is not a general criterion about how to choose the optimal wavelet basis function. In general, we choose a proper wavelet basis function by considering the properties of the wavelet basis function, features of signal to be analyzed and actual problem. The part of the signal whose shape is similar to that of the wavelet basis function will be enlarged, and other parts of the signal will be suppressed. In addition, proper scale wavelet is used according to the real problems. Big scale wavelet basis function should be used if we describe the total and approximate properties of the signal by the wavelet transform. Small scale wavelet basis function should be used if we extrude the details of the signal by the wavelet transform. Because the properties of the wavelet basis function reflect the analyzing ability to the signal, the wavelet basis function should be chosen by following criterions:

(1) Orthogonality: the coefficients of the orthogonal wavelet transform contain the least redundant information.
(2) Regularity: it is used to describe the smooth extent of a function. The smoother a function is, the higher its regularity is. Good regularity means good reconstructing results. However, some details of a signal may be lost if the regularity of the wavelet basis function is too good.
(3) Compact branch set: it can be sure the wavelet basis function to perform good time-frequency properties. The better the local properties of the wavelet is, the shorter the compact branch set is.
(4) Symmetry: symmetry can reflect if the filter properties of the wavelet has linear phase, which is related to distortion. Symmetric or anti-symmetric wavelet basis function should be used in order to reconstruct the signal.
(5) Vanishing moments: the rank of vanishing moment can be used to describe the focusing extent of the energy after wavelet transform. The better the details of a signal in the wavelet domain is extrude, the bigger the rank is.

We will use the CWT to detect the singularity of the curvature curve, so we should choose proper wavelet, which has similar shape to the signal to the analyzed, short compact branch set and big vanishing moment, as wavelet basis function. Some representative wavelet basis functions include: Coiflet, Symlets, Daubechies, Morlet, Mexihat and Meyer. Figure 4(a)–(f) show their function curves in time domain. According to Fig. 4 and Figs 2 and 3, we can see that the shapes of Meyer, Morlet, Coiflet and Symlet are similar to that of the curvature curve to be analyzed in Fig. 2 (1800–750 cm^{-1}). Compared to other three wavelets, Morlet wavelet has the shortest compact branch set (Fig. 4(c)), so we choose Morlet wavelet as analyzing wavelet.

In this paper the continuous wavelet transform is done to the FTIR spectra of *Stephania tetrandra* S. Moore and *Stephania cepharantha* Hayata's respectively, and the number of decomposing level is set as 15. Figure 5 shows the FTIR spectra and continuous wavelet coefficients of *Stephania tetrandra* S. Moore and *Stephania cepharantha* Hayata's in the region of 1800–750 cm^{-1}. If we choose L1–L4, it is very difficult to extract representative features in the small scale in the CWT domain because the detail signal is too sensitive to tinny changes of the spectrum characteristic peaks to result in some false features. Therefore, we should choose big scale to extract the features of the FTIR. We choose representative three levels (L5, L9 and L13) to extract their characteristics because the remaining levels have the similar characteristics to the three levels. Characteristic variable is defined as the energy of spectrum at scale 13, 9 and 5 in the continuous wavelet domain.

According to Fig. 5, we can see that the differences of CWT coefficients between *Stephania tetrandra* S. Moore and *Stephania cepharantha* Hayata's is obvious in three regions (1800–1300 cm^{-1},

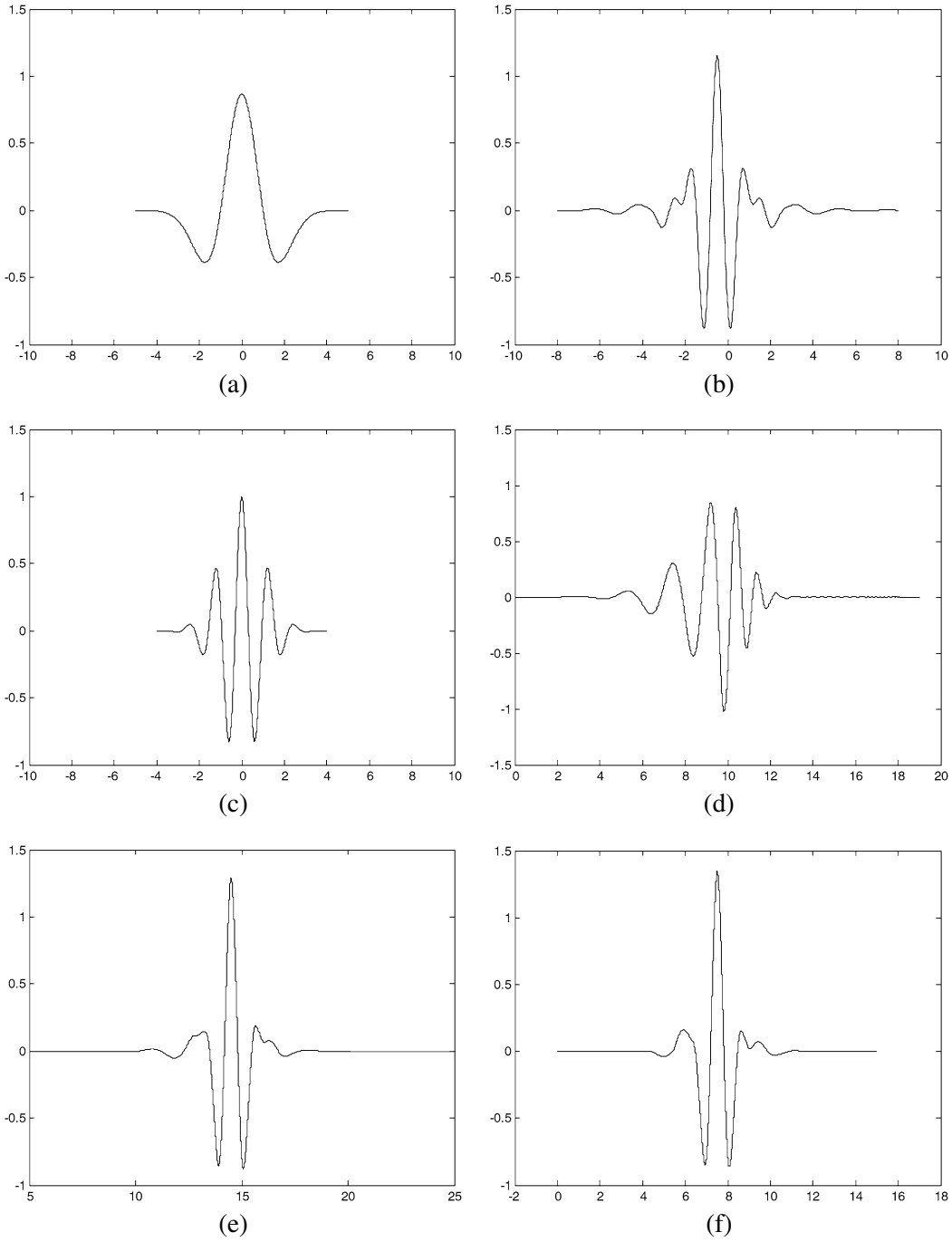

Fig. 4. Wavelet basis function curves in time domain. (a) Mexihat wavelet; (b) Meyer wavelet; (c) Morlet wavelet; (d) Db10 wavelet; (e) Coiflet5 wavelet; (f) Sym8 wavelet.

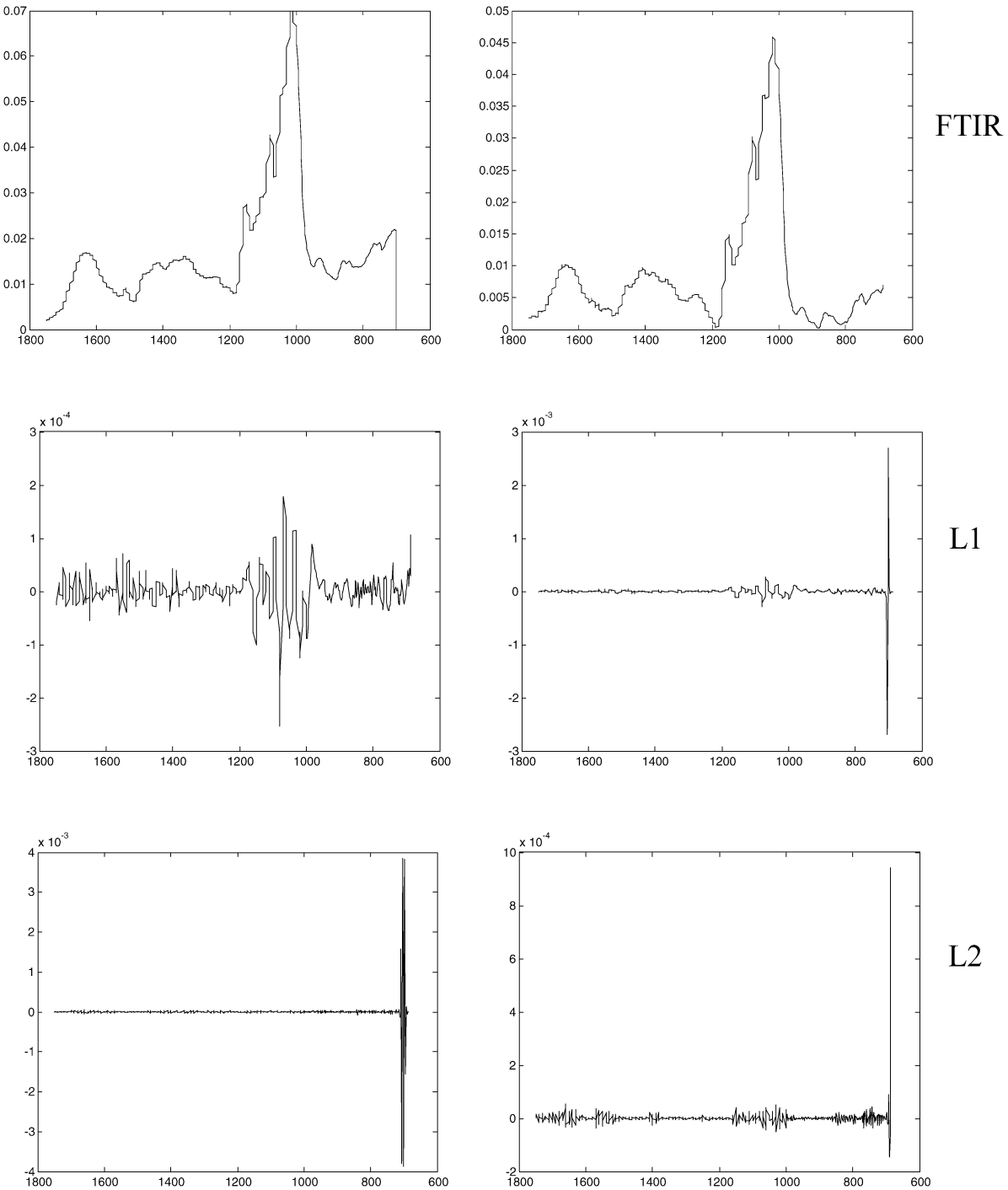

Fig. 5. FTIR (first row) and its continuous wavelet coefficients (second row to sixteenth row: L1–L15) of *Stephania tetrandra* S. Moore (left column) and *Stephania cepharantha* Hayata (right column).

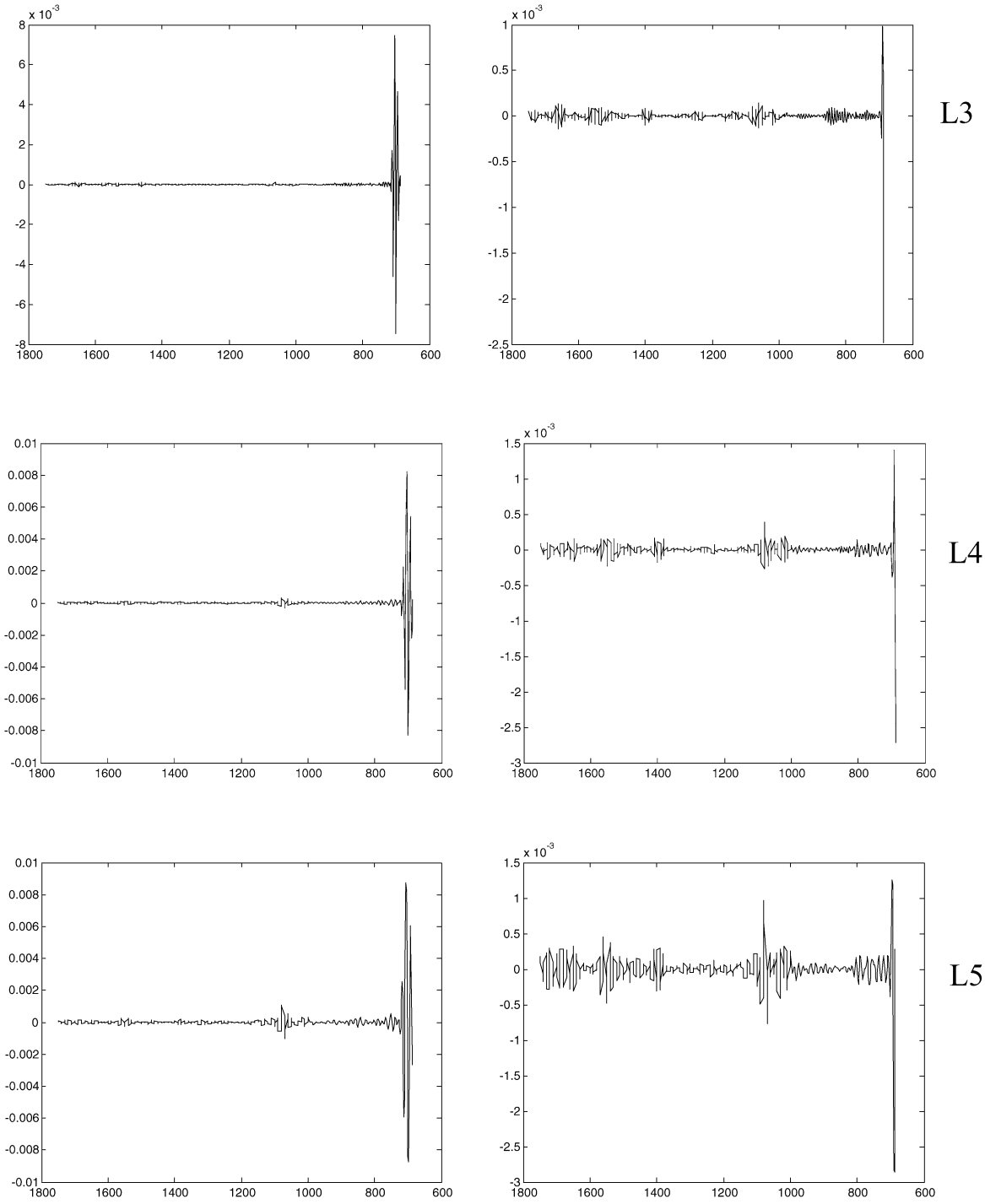

Fig. 5. (Continued).

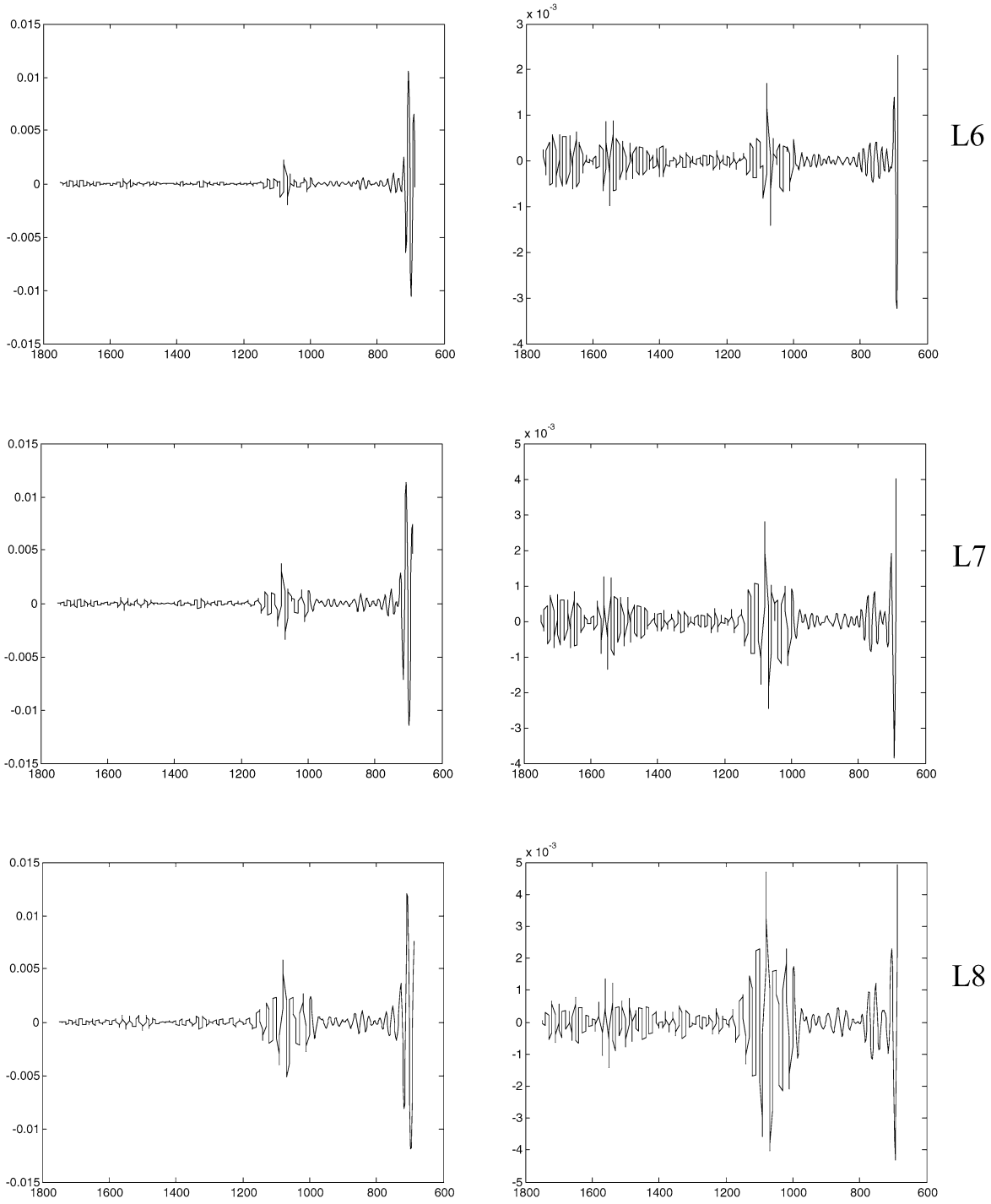

Fig. 5. (Continued).

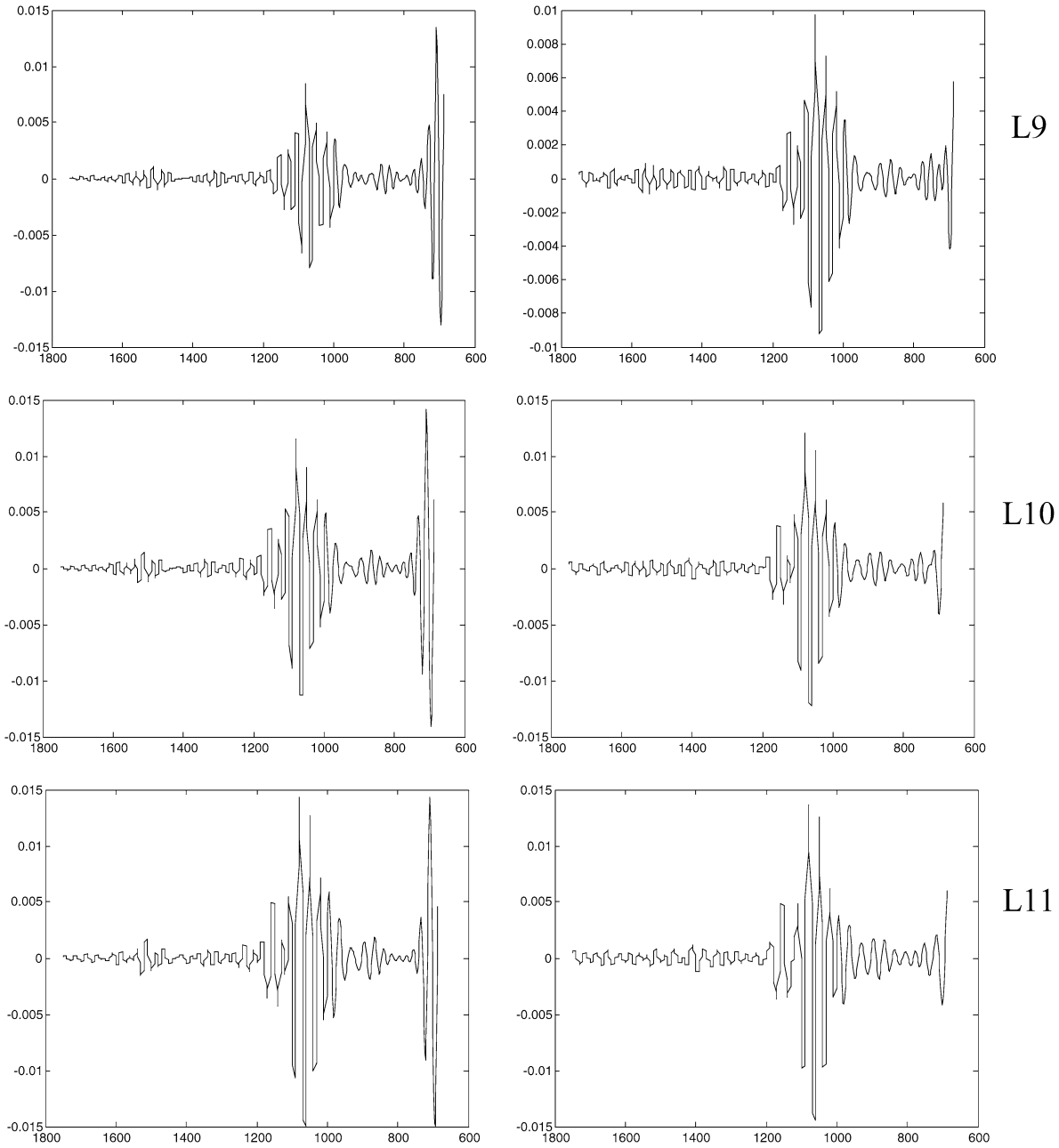

Fig. 5. (Continued).

1200–1100 cm^{-1} and 900–750 cm^{-1}). In order to effectively extract representative characteristics within three scales of continuous wavelet, the spectra in each scale is divided into three representative regions respectively. Figure 6 is the division diagram of the feature regions.

From Fig. 6 we can see that the region of 1800–750 cm^{-1} can be divided into three feature regions: 1800–1300 cm^{-1}, 1200–1100 cm^{-1} and 900–750 cm^{-1}. Nine feature regions of three scales in the CWT domain, whose feature values are the spectra energy in the nine feature regions, form the feature vector.

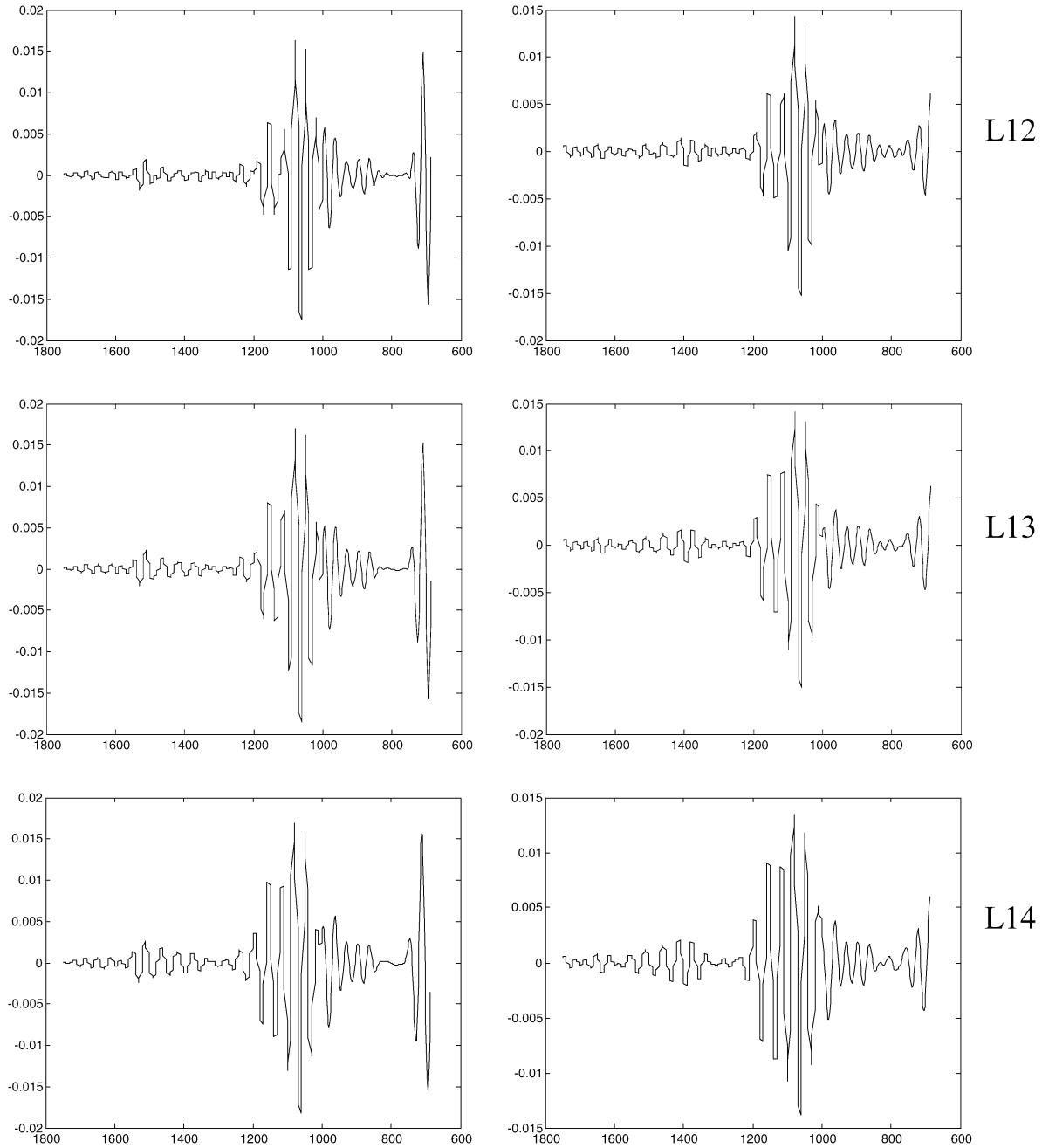

Fig. 5. (Continued).

4.4. Classification results

In order to verify the validity of proposed method, we test our method using the FTIR spectra of 128 pairs of *Stephania tetrandra* S. Moore and *Stephania cepharantha* Hayata's. Where 78 pairs of samples are used to train RBF neural network, and the remaining 50 pairs of samples are used to test the

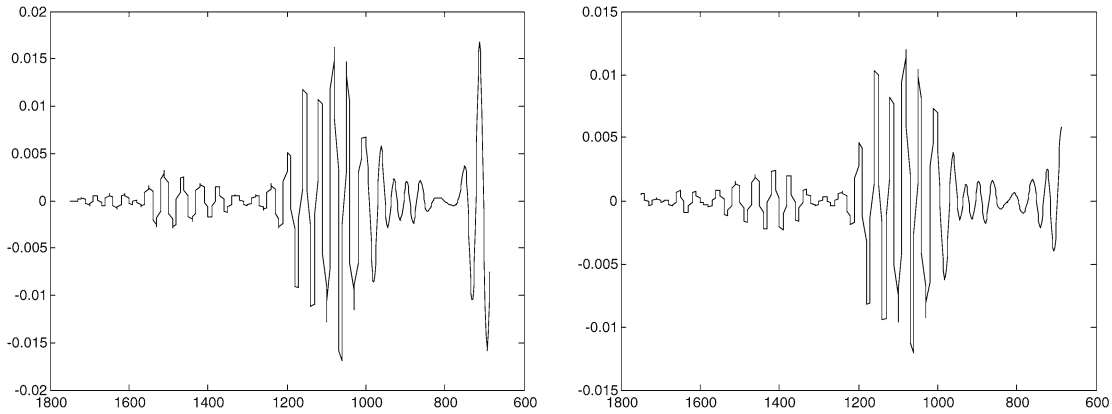

Fig. 5. (Continued).

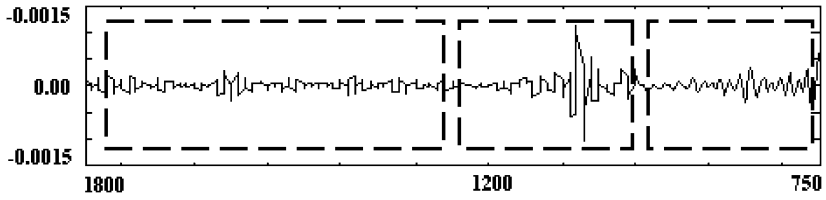

Fig. 6. Division of feature region in the CWT domain.

Table 1
Training and testing results by RBF neural network

Sample type	Identification rate of *Stephania tetrandra* S. Moore (%)	Identification rate of *Stephania cepharantha* Hayata's (%)
Training samples (78 pairs)	100	100
Testing samples (50 pairs)	99.8	99.9

performance of neural network. Table 1 shows the training and testing results by RBF neural network.

From Table 1 we can see that the identification rate with RBF neural network to identify the *Stephania tetrandra* S. Moore and *Stephania cepharantha* Hayata's is 100%, while testing samples of the identification rate is 99.8 and 99.9%, respectively. So the *Stephania tetrandra* S. Moore and *Stephania cepharantha* Hayata's can be correctly identified by combining RBF neural network with continuous wavelet features.

5. Conclusion

Direct determination of plant samples by FTIR is convenient and fast. The proposed method has a high recognition rate to the *Stephania tetrandra* S. Moore and *Stephania cepharantha* Hayata's by combining RBF neural network with the continuous wavelet features of FTIR of samples. Further work includes:

(1) Use other intelligent technique, for example, support vector machine (SVM) to replace RBF neural network to deal with similar problems.

(2) Some other features, for example, fractal features should be combined with the CWT features to form the feature vectors so as to improve the accurate identification rate.

References

[1] C.-G. Cheng, C.-R. Sun and Y.-J. Pan, *Spectroscopy and Spectral Analysis* **24** (2004), 1055–1059.
[2] C.-G. Cheng , Y.-M. Ruan and B.-L. Li, *Spectroscopy and Spectral Analysis* **24** (2004), 1355–1358.
[3] H. Wang, S.-Q. Sun and J.-W. Xu, *Spectroscopy and Spectral Analysis* **23** (2003), 253–257.
[4] C.-G. Cheng, *Spectroscopy and Spectral Analysis* **23** (2003), 282–284.
[5] Z. Wang, S.-Q. Sun and X.-B. Li, *Spectroscopy and Spectral Analysis* **21** (2001), 311–313.
[6] F. Ehrentreich, *Analytical and Bioanalytical Chemistry* **372** (2002), 115–121.
[7] L. Shao, X. Lin and X. Shao, *Applied Spectroscopy Reviews* **37** (2002), 429–450.
[8] Y.B. Ying, L. Yande, F. Xiaping and L. Huishan, *Proceedings of the SPIE – The International Society for Optical Engineering* **5587** (2004), 29–41.
[9] N. Lei, W. Shouguo, L. Xiangqin, Z. Longzhen and R. Lei, *Journal of Chemical Information and Computer Sciences* **42** (2002), 274–283.
[10] T. Khayamian, R. Tabaraki and A.A. Ensafi, *Journal of Molecular Graphics & Modelling* **25** (2006), 46–54.
[11] P.L. Piotrowski, B.G. Sumpter, H.V. Malling, J.S. Wassom, P.Y. Lu, R.A. Brothers, G.A. Sega, S.A. Martin and M. Parang, *Journal of Chemical Information and Modeling* **47** (2007), 676–685.
[12] F.-S. Yang *Engineering Analysis and Application of Wavelet Transform*, Science Press, Beijing, 2003.
[13] C.-J. Zhang and C.-G. Cheng, *Rare Metal Materials and Engineering* **35** (2006), 614–616.
[14] C.-J. Zhang, D.-T. Li, J.-Z. Liang and C.-G. Cheng, *Spectroscopy and Spectral Analysis* **27** (2007), 50–53.
[15] Y.-H. Peng, *Wavelet Transform and Its Engineering Application*, Science Press, Beijing, 2000.
[16] K.S. Jamuna, K.B. Dipak and N. Mita, *Applied Soft Computing* **7** (2007), 58–70.